THE JOURNAL OF PHYSICAL CHEMISTRY B LETTERS

2006, *110,* 23623−23627
Published on Web 11/09/2006

Conformational Selectivity of Peptides for Single-Walled Carbon Nanotubes

Zhengding Su, Tong Leung, and John F. Honek*

Department of Chemistry, University of Waterloo, Waterloo, ON N2L 3G1, Canada

Received: September 7, 2006; In Final Form: October 12, 2006

Carbon nanotubes show promising prospects for applications ranging from molecular electronics to ultrasensitive biosensors. An important aspect to understanding carbon nanotube properties is their interactions with biomolecules such as peptides and proteins, as these interactions are important in our understanding of nanotube interactions with the environment, their use in cellular systems, as well as their interface with biological materials for medical and diagnostic applications. Here we report the sequence and conformational requirements of peptides for high-affinity binding to single-walled carbon nanotubes (SWNTs). A new motif, $X_1THX_2X_3$-$PWTX_4$, where X_1 is G or H, X_2 is H or D or null, X_3 is null or R, and X_4 is null or K, was identified from two classes of phage-displayed peptide libraries. The high affinity binding of the motif to SWNTs required constrained conformations which were achieved through either the extension of the amino acid sequence (e.g., LLADTTHHRPWT) or the addition of a constrained disulfide bond (e.g., CGHPWTKC). This motif shows specific high-affinity to the currently studied SWNTs, compared to previously reported peptides. The conformations of the identified peptides in complex with SWNTs were also characterized with a variety of biophysical methodologies including CD, fluorescence, NMR spectroscopy, and molecular modeling.

Introduction

Single-walled carbon nanotubes (SWNTs) have potential biological applications ranging from biomedical sensors to tissue supports to drug delivery.[1−4] Recently the design and utilization of polypeptides specifically binding to carbon nanotubes (CNTs) has been the focus of much attention due to their functionality in biological systems.[5−10] Two research groups have shown that various peptides can bind different carbon nanotubes such as multiwalled nanotubes (MWNTs) and single-walled nanohorns (SWNHs) selected through phage libraries,[11,12] suggesting peptides as a potential means to overcome two major obstacles limiting the potential applications of CNTs, i.e., conformational heterogeneity and hydrophobicity. The peptides binding to MWNTs have consensus binding sequences rich in histidine and tryptophan at specific locations.[11] Molecular simulations show the peptides have condensed conformation probably driven by hydrophobic forces. The peptides binding to SWNHs have different amino acid sequences, and circular dichroism (CD) analysis revealed that these sequences display α-helical conformations driven by electrostatic forces.[12] However, the exact nature of biological-nanotube interactions is less well known, and this knowledge will be important in understanding their environmental and biological activity as well as their potential for application to nanostructure fabrication.

Several questions need to be addressed concerning affinity-selected peptide−nanotube interactions. For example, are there only one or two binding sequences that are selectable for related nanotubes (SWNTs and MWNTs) and nanohorns? How does the type of carbon-based nanomaterial differ in their selection for peptide sequence from a sequence library such as phage display? Do peptide sequences selected for one type of nanomaterial such as nanohorns maintain high affinity to other forms such as SWNTs? If primary sequence can vary within this recognition space for carbon-based nanomaterials, is there also a preferred peptide conformation that is optimal for these interactions?

As an initial step to explore these critical questions, three classes of phage libraries defined by length and constrained conformation were screened against SWNTs. Theoretically, a phage display peptide library with 20^n sequences would be required to cover all possible *n*-mer sequences. Since conventionally only $10^{10} \sim 10^{11}$ plaque-forming units (pfu) of phage are frequently used,[11−16] the coverage of all possible *n*-mer sequences becomes very low when $n > 7$ (e.g., $\sim 2.4 \times 10^{-4}$%, when $n = 12$); however, longer peptides provide more potential contacts with targets. In contrast, the coverage is almost 100% if a short peptide library (e.g., 7-mer) is used. In addition, introduction of disulfides into peptide libraries constrains conformational flexibility of displayed peptides, enhancing peptide binding affinity. Considering these and other factors, it was of interest to explore new SWNT-binding peptides using a variety of phage display libraries which has not previously been undertaken. In these constructed peptide libraries, peptides (12-mers, 7-mers, or disulfide-constrained 7-mers) are displayed on the surface of M13 phage by fusion to the N-terminal of pIII, a coat protein of this bacteriophage. Multiple binding/elution/amplification cycles with increasingly stringent conditions (i.e., Tween-20) enrich the pool in favor of the tightest binding sequences. The binding affinity and specificity of identified phage and peptides were quantitated and compared with previously reported peptide sequences having affinity to other

* Corresponding author. E-mail: jhonek@uwaterloo.ca. Tel: 519-888-4567 x35817; Fax: 519-746 0435.

10.1021/jp065837g CCC: $33.50

TABLE 1: Occurrence of Peptide Sequences Selectively Binding to SWNTs via Biopanning with Peptide Phage Display Libraries against Different Concentrations of Tween-20

PH.D.-12			PH.D.-C7C		
phage	sequence	occurrence	phage	sequence	occurrence
		$C_{Tween-20} = 1.0\%$			
UW−1	LLADTTHHRPWT	12/30	UW-4	CGIHPWTKC	12/28
UW−2	EHMALTYPFRPP	5/30	UW-5	CGRWGHIPC	5/28
		$C_{Tween-20} = 0.75\%$			
UW−3	ATNAPRYTMQWS	5/15	UW-6	CHTHNPWTC	3/15
	EHMALTYPFRPP	3/15			
		$C_{Tween-20} = 0.5\%$			
	LLADTTHHRPWT	3/10	UW-7	CHTHPWTKC	3/11

types of nanotubes. As we show, there exist multiple conformations for nanotube-binding peptides, strongly suggesting that the phage are selective toward their respective targets not only by sequence discrimination but also by conformational discrimination.

Experimental Methods

Three M13 phage-peptide libraries (Ph.D-12, Ph.D-C7C, and Ph.D-7, New England BioLabs) were subjected to biopanning of peptides for SWNTs (Cat # 652512, Lot # 09310HD, Sigma-Aldrich). SWNTs (1 mg/mL) were suspended by sonication using a Branson Sonifier 200 sonicator (Danbury, CT) equipped with a 4 mm diameter microtip in TBS buffer containing 0.1% Tween-20. Each phage library was preincubated with a graphite (Alfa Aesar, Ward Hill, MA, Cat #: 14734, Lot #: D02P23) suspension to minimize the isolation of graphite-selective phage. Panning experiments were initiated by mixing the recovered phage with the SWNT suspension. Unbound phage were removed by washing with TBS buffer containing the same concentration of Tween-20. Bound phage were eluted by incubating the particles with 2 M glycine-HCl (pH 2.2), immediately followed by neutralization. The eluted phage were amplified and subjected to the next round of biopanning. Biopanning was repeated six times with increasing Tween-20 concentrations (i.e., 0.2, 0.3, 0.4, 0.5, 0.75, and 1.0%). Phage particles randomly selected from the last three panning steps were characterized by DNA sequencing with the universal primer 96 gIII (NEB).

Binding affinity of selected peptides to SWNTs was quantitated by two different methods. (1) The binding affinity was measured in whole phage particles and defined by the standard protocol of the number of plaque-forming units in the binding pool.[11,17] (2) The binding affinity was also determined by measuring the amount of protein (or peptide) binding to SWNTs as the MFH-fusion proteins (see Supporting Information).

All the peptides were prepared by standard recombinant DNA techniques described previously.[18,19]

Circular dichroism (CD) was performed on free peptides in solution or in the presence of SWNTs using a Jasco J-715 spectropolarimeter (Easton, MD). Peptides were dissolved in TBS buffer (pH7.5) at a concentration of 6∼20 μM. The spectra were measured between 195 and 270 nm as the average of ten successive scans with a bandwidth of 1.0 nm and a scan speed of 20 nm/min. Steady-state tryptophan fluorescence measurements were made with a PTI QuantaMaster model QM-4/2005 (Birmingham, NJ). Samples were dissolved in TBS buffer (pH 7.5) at a concentration of 2∼10 μM. Excitation was set at 289 nm, the emission fluorescence spectra were measured between 300 and 550 nm with a scanning speed of 150 nm/s and an excitation slit of 1.0 nm.

Results and Discussion

In order to eliminate phage-displayed peptides that can interact with normal graphite, biopanning was initially done against graphite, producing a starting phage library free of graphite-binding phage. Subsequent biopanning under increasingly stringent conditions of detergent resulted in several consensus sequences being isolated. Table 1 shows the "graphite-free" phagotope sequences selected against SWNTs. With a 12-mer peptide library, several identical sequences occurred in high frequency when the detergent (i.e., Tween-20) concentration was increased to 0.5%. With further increasing Tween-20 concentrations, several identical sequences became more enriched. The amino acid sequence of LLADTTHHRPWT (i.e., UW-1) frequently appeared at 0.5% Tween-20 (3 out of 10) and at 1.0% Tween-20 (12 out of 30). Two other sequences, EHMALTYPFRPP (i.e., UW-2) and VLPPKPMRQPVA, were found at 0.75% Tween-20, and these sequences also appeared at a higher detergent concentration (i.e., 1.0% Tween-20) in relatively high frequency. The sequence of ATNAPRYTMQWS (i.e., UW-3) occurred frequently at 0.75% Tween-20 (5 out of 15), but it was not detected at other detergent concentrations. With a

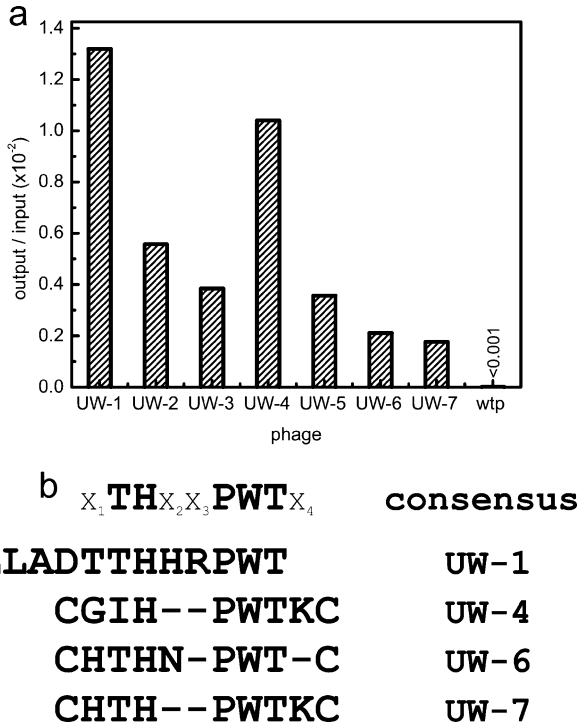

Figure 1. Summary of SWNT-binding peptide sequences chosen from two phage display libraries. (a) Binding affinities of seven screened phage to SWNTs. The binding affinity of the wild-type phage (i.e., wtp) was also determined as a control. (b) A consensus sequence was deduced from the above peptide sequences, where X_1 is G or H, X_2 is H or A or null, X_3 is null or R, and X_4 is null or K.

TABLE 2: Comparison of the Binding Affinity of Different Phage Displayed Peptides to SWNTs

peptide	amino acid sequence	phage method	fusion protein method	
		0.3%Tween-20 output/input × 10^{-2} (%)	0.1% Tween-20 (mmol/mg CNT)	0.3%Tween-20 (mmol/mg CNT)
B4[a]	HNWYHWWMPHNT	0.41 ± 0.06	3.53 ± 0.6	3.49 ± 0.7
B3[a]	HWSAWWIRSNQC	0.12 ± 0.04	1.78 ± 0.5	1.54 ± 0.6
ϕNH-12-5-2[b]	DYFSSPYYEQLF	0.25 ± 0.02	3.16 ± 0.7	3.08 ± 0.6
ϕUW-1	LLADTTHHRPWT	1.32 ± 0.12	6.21 ± 0.6	6.17 ± 0.8
ϕUW-4	CGIHPWTKC	1.04 ± 0.11	1.10 ± 0.4 (*Re*)[e]	0.47 ± 0.4
			4.92 ± 0.5 (*Ox*)*e*	4.67 ± 0.6
M13KE[c]		0.001	n/a	n/a
MFH[d]		n/a	0.04 ± 0.01	nd

[a] From ref 11. [b] From ref 12. [c] M13 phage without insert. [d] Fusion carrier protein. [e] Re and Ox denote reduced and oxidized state of the peptide, respectively; n/a: not available; nd: not detectable.

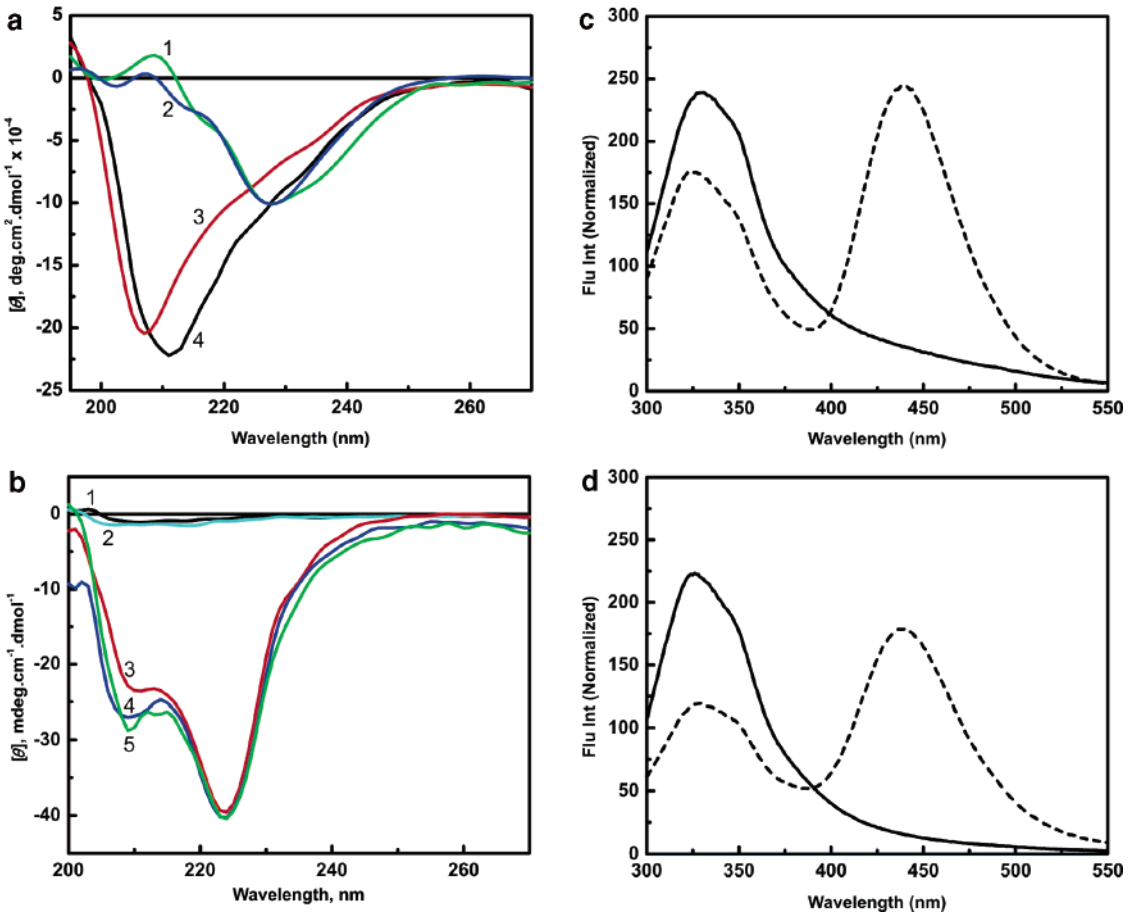

Figure 2. Conformational analysis of SWNT-binding peptides. (a) CD spectra of UW-1 peptide. Curve 1: UW-1 peptide (6 μM) in complex with SWNTs at pH 7.5. Curve 2: UW-1 peptide (12 μM) with SWNTs at pH 7.5 and the concentration of SWNTs is also doubled compared to that of curve 1. Curve 3: UW-peptide at pH 7.5. Curve 4: UW-1 peptide at pH 3.0. (b) CD spectra of B3 peptide. Curve 1: 1xTBS buffer. Curve 2: SWNTs in 1x TBS buffer. Curve 3: B3 peptide (18 μM) at pH 7.5. Curve 4: B3 peptide (6 μM) at pH 7.5. Curve 5: B3 Peptide (6 μM) in complex with SWNTs at pH 7.5. (c, d) The fluorescence emission spectra of the fusion protein, MFH−UW-1, in the absence or in the presence of SWNTs (solid lines). Substantial fluorescence energy transfer occurs when Pro-Q Sapphire 365 dye was added, as indicated by the large emission intensity in the vicinity of 450 nm on excitation of the tryptophan at 289 nm (dash lines).

disulfide-constrained 7-mer phage peptide library, the sequence CGIHPWTKC (i.e., UW-4) had higher occurrence at the higher detergent concentrations (3 out of 15 and 12 out of 28 at 0.75% and 1.0% Tween-20, respectively). In contrast, with a 7-mer unconstrained peptide phage library, no consensus sequence could be found at detergent concentrations from 0.5% to 1.0 and no sequence identical to the above sequences was obtained (data not shown).

As shown in Figure 1a, two phage (i.e., UW-1 and UW-4, Table 1) of seven selected phage (i.e., UW-1, UW-2, UW-3, UW-4, UW-5, UW-6, and UW-7) show higher binding affinities to SWNTs than other phage. Based on these amino acid sequences, a consensus sequence could be deduced: $X_1THX_2X_3$-$PWTX_4$, where X_1 is G or H, X_2 is H or D or null, X_3 is null or R, and X_4 is null or K (Figure 1b).

It was of interest to compare the binding affinity of these two newly isolated SWNT-binding peptides with three previously identified phage-displayed sequences (i.e., B3, B4, and ϕNH-12-5-2)[11,12] which have been previously isolated from screening against MWNTs and SWNHs respectively, because those peptides contain different amino acid sequences and positions of key His and Trp residues. Two newly isolated phage, i.e., UW-1 and UW-4, show stronger binding affinity to the current SWNTs than previously reported phage peptide sequences (Table 2). With the assay buffer containing 0.3% Tween-20, UW-1 and UW-4 (Ox) phage had ratios of output/

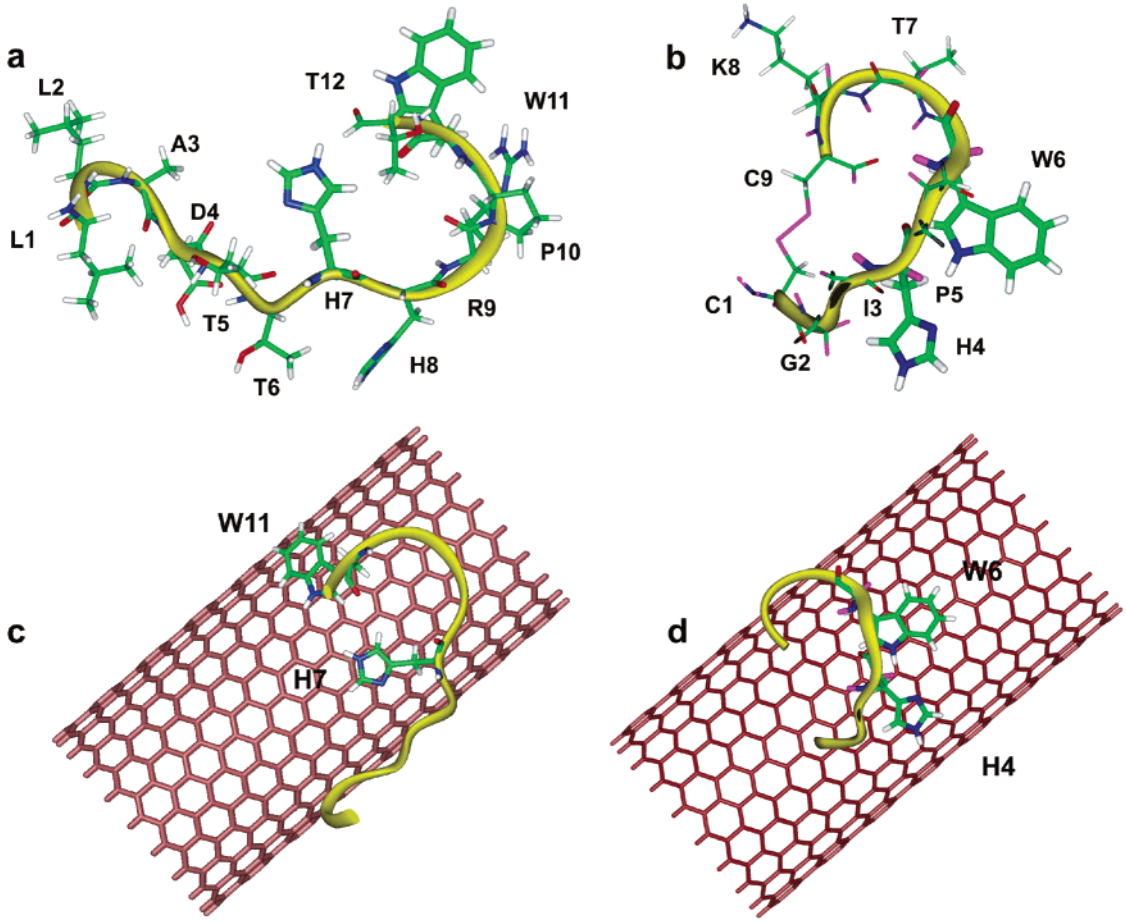

Figure 3. Molecule modeling of two SWNT binding peptides. Low-energy conformations of UW-1 (a) and UW-4 (b) peptides are in β-turn like structures forming a unique surface for SWNT binding. This representation of the peptide conformation was prepared using the Insight II program (Accelrys, San Diego, CA). Possible orientations of UW-1 (c) and UW-4 (d) peptides interacting SWNTs are shown on the surfaces of SWNTs, suggesting interactions of the rings from tryptophan and histidine with the surfaces of SWNTs.

input (see Experimental Methods) of 1.32 ± 0.12% and 1.04 ± 0.11%, respectively, whereas the other phage including B3, B4, and ϕNH-12-5-2 had ratios of output/input below 0.41 ± 0.06%. When these five peptides were fused to a soluble fusion carrier protein (i.e., MFH, see Supporting Information), they could be directly utilized to determine binding selectivity to SWNTs as nonspecific binding caused by the fusion carrier could be completely eliminated when a higher concentration of Tween-20 was applied (e.g., 0.3%). When MFH-fusion proteins were used, the observed results were consistent with those found by phage-titration (Table 2). The binding affinities of the MFH-fusion proteins of UW-1 and oxidized UW-4 were found to be higher than the others and were determined to be 6.17 ± 0.8 and 4.67 ± 0.6 mmol/mg SWNTs in the presence of 0.3% Tween-20, respectively. As indicated in Table 2, the reduced UW-4 MFH-fusion protein exhibited lower binding affinity, i.e., 1.10 ± 0.4 mmol/mg SWNT (in 0.1% Tween-20) and 0.47 ± 0.06 mmol/mg SWNT (0.3% Tween-20). Nevertheless, the binding of the reduced UW-4 MFH-fusion protein to SWNT was specific.

To characterize the structural features of the UW-1 peptide in complex with SWNTs, circular dichroism (CD) spectroscopy was used to investigate the UW-1 free peptide and, for comparison, the B3 free peptide under various conditions. As shown in Figure 2a, the UW-1 peptide exhibits a β-sheet-like conformation at low pH. It adopts a random coil conformation at neutral pH; however, it changes into a β-turn (or β-hairpin) structure when bound to SWNTs in solution. This is not observed for other carbon nanotube (MWNT and SWNH) binding peptides.[11,12] On the other hand, the free B3 peptide with affinity to MWNTs has a helical conformation at neutral pH and binding to the current SWNTs does not affect this conformation (Figure 2b). This conformational feature measured by CD is totally different from the conformation prediction by computer simulation.[11] In addition, the conformation of both the UW-1 and B3 free peptides are different from that of SWNH-binding peptide (i.e., NH-12-5-2) in solution in the absence or in the presence of SWNHs.[12]

In an attempt to define the end-to-end distance of the β-hairpin structure of the UW-1 peptide in complex with SWNTs, we utilized the MFH-fusion protein construct with the UW-1 peptide, especially an MFH−UW-1 fusion protein consisting of a 6xHis-tag adjacent to the N-terminus of the UW-1 peptide (see Figure S2, Supporting Information), which could be used to specifically attach a fluorescence probe (Pro-Q Sapphire 365 (Molecular Probes)) which contains a nickel nitrilotriacetic acid (Ni-NTA) moiety and has affinity to His-tag protein sequences. When this probe was added in slight access (protein/dye = 1:1.20) to the fusion protein in the absence of nanotubes, a fluorescence resonance energy transfer (FRET) occurred as shown in Figure 2c. The FRET efficiency was approximately 0.31, which was translated into a donor−acceptor distance of 31.8 Å, suggesting the conformation of the UW-1 peptide fragment in the MFH-fusion protein in the absence of SWNTs is in an opened form, as the theoretical value of this distance is ~40.6 Å in an extended model (modeling not shown).

However, in the presence of SWNTs, the FRET was more pronounced ($E = 0.67$, Figure 2d) than that in the absence of SWNTs, resulting in a reduced distance of the Trp-Sapphire 365 pair (~13.5 Å). This is interpreted as induction of a folded structure in the UW-1 peptide upon interaction with SWNTs. The folded conformation may be driven by a spatial clustering of aromatic and hydrophobic residues with favorable orientations to promote stacking interactions with the nanotube surface. Moreover, this proximity between the two peptide termini supports the aforementioned β-turn structure.

The conformational analysis of the peptide was computed based on aforementioned experimental observations: (1) the existence of a β-turn structure induced by SWNT-binding as determined by CD; (2) the close end-to-end solution structure measured by FRET, and (3) the close end-to-end conformation defined by the disulfide bond in the disulfide constrain sequence (e.g., the UW-4 peptide). Figures 3a and 3b show low-energy conformations for UW-1 and UW-4 free peptides as calculated by energy minimization and molecular dynamics, respectively. Each folded structure of two binding peptides shows a spatial clustering of aromatic and hydrophobic residues with favorable orientations to promote stacking interactions with a SWNT surface (Figure 3c and 3d). Interestingly, one could expect that the formation of a β-turn structure may cluster hydrophobic residues, forming hydrophobic surface(s) favorable for SWNT-binding. Although the detailed driving force(s) for SWNT-binding at the molecular level still remains elusive, it is likely that hydrophobic interactions as well as $\pi-\pi$ interactions between the sidechain of aromatic residues and the surface of SWNTs play important roles (e.g., W11 and H7 in UW-1 peptide, and W6 and H4 in UW-4 peptide in Figure 3).

Conclusion

In summary, we have identified a new peptide motif, X_1-$THX_2X_3PWTX_4$, where X_1 is G or H, X_2 is H or D or null, X_3 is null or R, and X_4 is null or K, from multiple phage libraries which, owing to constrained conformations, exhibits selective binding to SWNTs, compared to previously reported peptides binding to other forms of nanotubes (multiwalled and nanohorns).[11,12] The identified peptides in complex with SWNTs show β-hairpin conformations which are achieved through either sequence extension or disulfide bond constraints. This unique feature has not been observed with other peptides, including designed nanotube-binding peptides.[5−7] It is interesting to question what structure on SWNTs the peptide motifs bind; in other words, how general is this sequence motif? A further detailed exploration with these peptides and phage for purification of SWNTs is currently being carried out. Nevertheless, the current work does reveal that different nanotube-binding peptides exhibit distinct and different conformations relevant to their binding selectivity, which provides a molecular basis to address emerging concerns on the interactions of biomolecules with SWNTs (see Introduction). These new findings may allow for the application of defined peptides to the purification and assembly of SWNTs in the future. On the other hand, these findings may have implications to environmental and toxicological aspects of these nanomaterials.[20−22] It is important to note that there are diverse solutions in nature to molecular recognition of xenomaterials such as SWNTs that depend on sequence as well as conformation of the biomolecule.

Acknowledgment. We thank NSERC NanoIP for financial support of this research and Dr. Nina Heinig and Amy Zhai for technical assistance.

Supporting Information Available: Materials and methods, results on binding assays, fluorescence spectroscopy, heteronuclear NMR spectroscopy, and molecular modeling. This material is available free of charge via the Internet at http://pubs.acs.org.

References and Notes

(1) Bianco, A.; Kostarelos, K.; Prato, M. *Curr. Opin. Chem. Biol.* **2005**, *9*, 674−679.
(2) Martin, C. R.; Kohli, P. *Nat. Rev. Drug Discovery* **2003**, *2*, 29−37.
(3) Li, J.; Ng, H. T.; Chen, H. *Methods Mol. Biol.* **2005**, *300*, 191−23.
(4) Contarino, M. R.; Sergi, M.; Harrington, A. E.; Lazareck, A.; Xu, J.; Chaiken, I. *J. Mol. Recognit.* **2006**, *19*, 363−371.
(5) Dieckmann, G. R.; Dalton, A. B.; Johnson, P. A.; Razal, J.; Chen, J.; Giordano, G. M.; Munoz, E.; Musselman, I. H.; Baughman, R. H.; Draper, R. K. *J. Am. Chem. Soc.* **2003**, *125*, 1770−1777.
(6) Ortiz-Acevedo, A.; Xie, H.; Zorbas, V.; Sampson, W. M.; Dalton, A. B.; Baughman, R. H.; Draper, R. K.; Musselman, I. H.; Dieckmann, G. R. *J. Am. Chem. Soc.* **2005**, *127*, 9512−9517.
(7) Zorbas, V.; Ortiz-Acevedo, A.; Dalton, A. B.; Yoshida, M. M.; Dieckmann, G. R.; Draper, R. K.; Baughman, R. H.; Jose-Yacaman, M.; Musselman, I. H. *J. Am. Chem. Soc.* **2004**, *126*, 7222−7227.
(8) Karajanagi, S. S.; Yang, H.; Asuri, P.; Sellitto, E.; Dordick, J. S.; Kane, R. S. *Langmuir* **2006**, *22*, 1392−1395.
(9) Pender, M. J.; Sowards, L. A.; Hartgerink, J. D.; Stone, M. O.; Naik, R. R. *Nano. Lett.* **2006**, *6*, 40−44.
(10) Bianco, A.; Hoebeke, J.; Kostarelos, K.; Prato, M.; Partidos, C. D. *Curr. Drug Deliv.* **2005**, *2*, 253−259.
(11) Wang, S.; Humphreys, E. S.; Chung, S. Y.; Delduco, D. F.; Lustig, S. R.; Wang, H.; Parker, K. N.; Rizzo, N. W.; Subramoney, S.; Chiang, Y. M.; Jagota, A. *Nat. Mater.* **2003**, *2*, 196−200.
(12) Kase, D.; Kulp, J. L., III; Yudasaka, M.; Evans, J. S.; Iijima, S.; Shiba, K. *Langmuir* **2004**, *20*, 8939−8941.
(13) Smith, G. P.; Petrenko, V. A. *Chem. Rev.* **1997**, *97*, 391−410.
(14) Smothers, J. F.; Henikoff, S.; Carter, P. *Science* **2002**, *298*, 621−622.
(15) Clackson, T.; Hoogenboom, H. R.; Griffiths, A. D.; Winter, G. *Nature* **1991**, *352*, 624−628.
(16) Matthews, D. J.; Wells, J. A. *Science* **1993**, *260*, 1113−1117.
(17) Dennis, M. R.; Lowman, H. B. *Phage Display A Practical Approach*; Oxford University Press: Oxford, 2004; pp. 61−84.
(18) Osborne, M. J.; Su, Z.; Sridaran, V.; Ni, F. *J. Biomol. NMR* **2003**, *26*, 317−326.
(19) Su, Z.; Vinogradova, A.; Koutychenko, A.; Tolkatchev, D.; Ni, F. *Protein Eng. Des. Sel.* **2004**, *17*, 647−657.
(20) Fiorito, S.; Serafino, A.; Andreola, F.; Togna, A.; Togna, G. *J. Nanosci. Nanotechnol.* **2006**, *6*, 591−599.
(21) Hardman, R. *Environ. Health Perspect.* **2006**, *114*, 165−172.
(22) Scott, N. R. *Rev. Sci. Technol.* **2005**, *24*, 425−432.